1 **The brain and the braincase: a spatial analysis on the midsagittal profile in adult humans**

2 Emiliano Bruner[1], Hideki Amano[2], José Manuel de la Cuétara[3], Naomichi Ogihara[2]

3

4 [1] Centro Nacional de Investigación sobre la Evolución Humana, Burgos (Spain)

5 [2] Keio University, Yokohama (Japan)

6 [3] Universidad Autónoma de Madrid, Madrid (Spain)

7

8 Corresponding author: Emiliano Bruner, Centro Nacional de Investigación sobre la Evolución
9 Humana, Paseo Sierra de Atapuerca 3, 09002 Burgos, Spain; email: emiliano.bruner@cenieh.es

10

11 **Abstract**. The spatial relationships between brain and braincase represent a major topic in
12 surgery and evolutionary neuroanatomy. In paleoneurology, neurocranial landmarks are often
13 used as references for brain areas. In this study, we analyze the variation and covariation of
14 midsagittal brain and skull coordinates in a sample of adult modern humans in order to
15 evidence spatial associations between hard and soft tissues. The correlation between parietal
16 lobe size and parietal bone size is very low, and there is a marked individual variation. The
17 distances between lobes and bones are partially influenced by the dimensions of the parietal
18 lobes. The main pattern of morphological variability among individuals, associated with the
19 size of the precuneus, does not influence apparently the position of the neurocranial sutures.
20 Therefore, variations in the precuneal size modify the distance between the paracentral lobule
21 and bregma, and between the parietal lobe and lambda. Hence, the relative position of the
22 cranial and cerebral landmarks can change as a function of the parietal dimensions. The scarce
23 correlation and covariation among these elements suggest a limited degree of spatial
24 integration between soft and hard tissues. Therefore, although the brain influences the cranial
25 size and shape during morphogenesis, the specific position of the cerebral components is
26 sensitive to multiple effects and local factors, without a strict correspondence with the bone
27 landmarks. This absence of correspondent change between brain and skull boundaries
28 suggests caution when making inferences on the brain areas from the position of the cranial
29 sutures. The fact that spatial relationships between cranial and brain areas may vary according
30 to brain proportions must be considered in paleoneurology, when brain anatomy is inferred
31 from cranial evidence.

32

33 **Keywords**: neuroanatomy, parietal lobes, precuneus, vault, geometric morphometrics,
34 paleoneurology;

35

36   **Introduction**

37

38   The brain and the braincase are partially integrated through their functional and structural
39   relationships (Richstmeier et al., 2006). Brain growth generates pressures during
40   morphogenesis, inducing changes on the elements of the braincase (Enlow, 1990). At the same
41   time, such forces may be redirected by biomechanical tensors like the meningeal layers (Moss
42   and Young, 1960) or, on a smaller scale, by the neurons themselves (Van Essen, 1997; Hilgetag
43   and Barbas, 2005), shaping the braincase and the cortex, respectively. The facial block and the
44   cranial base exert further constraints on the neurocranial and cerebral system, adding further
45   factors of correlation (Bookstein et al., 2003; Bastir and Rosas, 2005). In ontogenetic terms, the
46   neural elements, maturing earlier, influence the basal and facial areas, which mature later
47   (Bastir et al., 2006). Nonetheless, later changes of the facial block can induce minor changes of
48   the brain morphology (Neubauer et al., 2009). In evolutionary terms, it is expected that the
49   bone components influence the brain morphology at the endocranial base, while in the vault
50   the reverse situation is more likely, with the cortical tissue shaping the bony elements (Bruner,
51   2015). Integration plays a major role in phylogenetic and ontogenetic changes, but it seems
52   somehow less decisive in shaping adult intra-specific variation. In adult variability, local factors
53   still have a major role in influencing the endocranial (Bruner and Ripani, 2008) and cerebral
54   (Bruner et al., 2010; Gomez-Robles et al., 2014) shape. In both cases, spatial proximity is the
55   main source of integration suggesting that, at least in morphology, structural factors may be
56   largely a matter of short range physical interactions. Such local influences and anatomical
57   dissociation are therefore major forces in cranial evolution (Bookstein et al., 2003;
58   Mitteroecker and Bookstein, 2008).

59   The spatial organization of brain and braincase is a relevant issue in medical and evolutionary
60   fields. In microsurgery, the spatial relationships between cranial and cerebral points can supply
61   relevant information during craniotomies and for intraoperative identification of the sulcal
62   patterns (Ribas et al., 2006). The reciprocal influence between soft and hard neurocranial
63   elements is also essential when dealing with pathological conditions altering the timing of
64   growth and development, like in craniosynostoses (Aldridge et al., 2002). In paleoneurology,
65   this information is necessary to provide reliable inferences on brain morphology from
66   neurocranial osteometric landmarks (Holloway et al., 2004; Bruner et al., 2011; Ogihara et al.,
67   2015). Previous analyses have been published which investigate the brain midsagittal shape
68   variation in adult humans by using digital anatomy and geometric morphometrics, this plane
69   being relevant in terms of biological organization and human evolution (Bruner et al., 2010;
70   2014a). However, we ignore how these brain morphological variations can influence the
71   boundaries of the cranial elements, and to what extend the cranial boundaries can be used to
72   get indirect information on the extension of the underlying brain areas.

73   The morphogenetic association between vault bones and lobes is due to brain pressure and
74   endocranial forces redistribution (Moss and Young, 1960; Enlow, 1990) and embryological
75   processes shared by soft and hard tissues (Jang et al., 2002; Morriss-Kay and Wilkie, 2005).
76   This leads to a correspondence between brain and bones general morphology and surface

77 geometry. Nonetheless, beyond the general vault curvature, we currently ignore to what
78 extent the expansion of the bone, as delimited by its sutures, is influenced by brain size.

79 The pattern of suture displacement will depend upon local factors and the precise distribution
80 of such morphogenetic forces (Fig. 1). A correspondent growth of lobes and bones will involve
81 proportional changes between these areas. In this case, for example, larger parietal lobes will
82 involve larger parietal bones, and a proportional displacement of the respective sutures.
83 Conversely, a non-linear growth, or a growth based on multiple independent factors, will
84 involve a small or null spatial correlation between cranial and cerebral elements.

85 To investigate these two alternatives, we analyze the spatial variations of midsagittal cranial
86 and cerebral landmarks in a sample of adult individuals in order to establish patterns and
87 constraints associated with the relationships between hard and soft tissues according to the
88 normal endocranial variability of our species. A null hypothesis is represented by absence of
89 association between bones and lobes, in terms of dimensions (as measured by diameters) and
90 spatial position (as measured by landmark coordinates). In this case, larger lobes are not
91 associated with larger bones, and the brain variations do not influence the dimensions of the
92 bones and the position of their sutures. Conversely, under a direct and linear relationship,
93 changes in one of these references (cranial bones or brain lobes) should be associated with
94 corresponding changes in the others. In this case, the spatial relationships between cranial and
95 brain landmarks should remain stable. If brain morphology influences directly the growth of
96 the adjacent bone elements, for example, larger parietal bones should be associated with
97 larger parietal lobes, and the spatial relationships between lobes and bones should remain
98 constant.

99

100 **Materials and methods**

101

102 One-hundred adult individuals were sampled from the OASIS magnetic resonance (MRI)
103 database (Marcus et al., 2007). The sample is composed of 50 males and 50 females, with an
104 age range of 20-40 years. This range was selected to include brains with full maturation and
105 stable cortical morphology (according to Gogtay et al., 2004), but avoiding the following
106 decades in which brain shrinking can influence the spatial relationships between brain and
107 skull topology. MRI signal is based onto the concentration of water or fat, and it is therefore
108 more suited to reveal the morphology of the soft tissues. Although it is scarcely useful to
109 reveal the cranial elements, it can however show the position of the cranial sutures, because
110 of their connective content (Cotton et al., 2005). Using MRI to reveal sutures and bone
111 boundaries can limit the resolution of the analysis, but nonetheless it represents a useful
112 operational compromise to deal with soft and hard tissues at once. Integration of tomographic
113 and resonance data would be more suited for this scope but, at present, it is not feasible for
114 large samples in terms of costs, logistics, and X-ray exposure. Because of the noise associated
115 with this operational limit, further researches with different techniques will be surely
116 necessary to supply more detailed data on this topic.

117   We analyzed the midsagittal section because it has many homologous landmarks for both
118   brain and skull, being largely investigated in evolutionary neuroanatomy (Bruner et al., 2004;
119   2010). Twenty-three landmarks were sampled in two dimensions from brain and cranial
120   references (Fig. 2). In particular, the boundaries between frontal, parietal, and occipital bones
121   and lobes are of interest for this study to evaluate whether the position of the former can be
122   used to estimate the position of the latter. Landmarks on the vault profile were all sampled
123   along the endocranial surface, independently upon the presence of meninges and of the
124   cerebrospinal fluid. Scans are below such degree of resolution, and this minor approximation
125   does not influence the macroanatomical variations we are interested in this study. Although
126   this study concerns the midsagittal elements, landmarks have been localized by using the
127   information available throughout the whole MRI stacks. This approach is useful when dealing
128   with individual variations, allowing the recognition on a larger scale of sulci and gyri beyond
129   confounding factors like the presence of connective and vascular components. Bregma
130   (endobregma) and lambda (endolambda) were localized by following, throughout the whole
131   MRI stacks, the course of the coronal and lambdoidal sutures. The sutures can be recognized
132   moving along the stacks through transversal or sagittal sections, and bregma and lambda can
133   be recognized as the midsagittal meeting point between the left and right sutures. The
134   position of the lambda compared to the location of the parieto-occipital sulcus and the
135   position of the bregma compared to the central sulcus were specifically considered, being
136   generally used to delimit the frontal, parietal, and occipital territories. Landmarks were
137   sampled by one single researcher (HA). Intra-observer error based on 5 replicas digitized in 5
138   independent sessions shows a range of 0.4 - 1.8 mm, averaging 0.8 mm. Distances between
139   bregma, central sulcus, marginal branch of the cingulate sulcus, lambda, and perpendicular
140   sulcus were quantified by studying the distributions of the their distances. The distance
141   between the marginal branch of the cingulate sulcus and the parieto-occipital sulcus
142   represents the length of the precuneus. This diameter is particularly important, considering
143   previous results on its variation (Bruner et al., 2014; Bruner et al., 2015). The distance between
144   bregma and lambda represents the length of the parietal bone. The distance between central
145   sulcus and parieto-occipital sulcus represents the length of the parietal lobe. The distance
146   between the central sulcus and bregma represents the overlapping area between parietal
147   bone and frontal lobes. The distance between lambda and the perpendicular sulcus represents
148   the overlapping area between parietal bone and occipital lobes. This last value can be
149   negative, considering that in few specimens the perpendicular sulcus can be positioned before
150   lambda, that is under the occipital bone. A preliminary analysis showed a strong correlation
151   between precuneus chord and arc (R = 0.997; p = 0.0001) and parietal bone chord and arc (R =
152   0.962; p = 0.0001). However, both arcs and chords will be used here as proxy of midsagittal
153   size for bones and lobes in order to take the effect of bulging into account.

154   First, an analysis based on linear correlation among bones and lobes lengths was aimed at
155   investigating the overall proportions between hard and soft elements. Second, a shape
156   analysis was performed to evaluate the role of the bones and lobes boundaries within the
157   main morphological correlation patterns. Shape variation, as represented by a geometrical
158   model based on landmark coordinates, was analyzed according to the principles of geometric
159   morphometrics (Zelditch et al., 2004). Two dimensional coordinates from 23 cerebral and

160   cranial landmarks (Figure 2) were normalized by Procrustes superimposition, by translating to
161   a common centroid, scaling to unitary centroid size, and rotated as to minimize the distance
162   between corresponding landmarks (Bookstein, 1991). This registration minimizes the spatial
163   differences within the sample, and the residuals after normalization are available to be
164   analyzed through multivariate statistics. Shape coordinates were analyzed by Principal
165   Component Analysis, to describe and quantify the patterns of covariation among the
166   transformed coordinates. The patterns of variation along the multivariate vectors can be
167   visualized by coordinate displacement and geometrical models, or by using deformation grids
168   based on thin-plate spline function, which interpolates the minimum deformation associated
169   with the differences between configurations or along multivariate axes. As such, shape
170   changes are strictly referred to relative proportions and spatial relationships, and not to the
171   overall dimensions.

172   Correlation between different groups of landmarks (blocks) was also further tested by Partial
173   Least-Square correlation based on separate superimpositions (Rohlf and Corti, 2000). Statistics
174   were computed with MorphoJ 1.06f (Klingenberg, 2011) and PAST 2.17 (Hammer et al., 2001).

175

176   **Results**

177

178   Table 1 shows the distribution of the distances between the main anatomical references.
179   According to these values, the precuneus length is definitely more variable (coefficient of
180   variation 20.6) than the parietal bone length (coefficient of variation 5.1). The correlation
181   between parietal lobe and parietal bone lengths is low (chords: R = 0.27; p = 0.01; arcs: R =
182   0.32; p = 0.001) and the correlation between precuneus length and parietal bone length is
183   even more modest (chords: R = 0.20; p = 0.05; arcs: R = 0.24; p = 0.02). Hence, although a
184   larger precuneus is associated with larger parietal bone, this relationship explains only
185   between 4% and 6% of the latter values, suggesting a considerable individual variation based
186   on different factors. When considering the whole parietal lobes, its correlation with the
187   parietal bone explains a little more (7%-10%). There is a moderate negative correlation
188   between the precuneus length and the separation of the boundaries between the parietal
189   bone and lobe (R = -0.37 and p = 0.0002 for both metrics, namely the distance between
190   bregma and central sulcus, and the distance between lambda and parieto-occipital sulcus).
191   Therefore, the larger the precuneus the more the boundaries of the lobe approach the
192   boundaries of the bone. This suggests that the extension of the bone is not much sensitive to
193   or associated with the extension of the lobe.

194   The scatterplot of the Procrustes coordinates (Fig. 2) shows that, although lambda generally
195   lies behind the parieto-occipital sulcus, there is some overlapping in the variations of these
196   two landmarks. In fact, in 10 specimens (10% of the sample), lambda, which is generally
197   located behind the parieto-occipital sulcus, was found to be positioned beyond it, and hence
198   the boundary between the parietal and occipital bone trespasses the boundary between the

199 parietal and occipital lobes. In contrast, bregma is always very far from the central and
200 precentral sulci, well above the prefrontal cortex.

201 A principal component analysis of the Procrustes coordinates shows a first dominant
202 component and a set of secondary components, showing only minor differences in their
203 relative weight (Fig. 3). According to a broken stick threshold based on random distribution,
204 and to a threshold of 5% of variance explained, at least the first six components are significant.
205 Such minor differences between these secondary components can be interpreted as the result
206 of the scarce morphological integration described in the skull (Bruner and Ripani, 2008) and
207 brain (Bruner et al., 2010; Gómez-Robles et al., 2014) as a whole, and will not be discussed
208 further. Because of the dominant role of the first component, only this vector will be evaluated
209 in detail, as a reliable biological pattern of covariation in this study. This first principal
210 component explains 25% of the variance, and it is associated with dilation/contraction of the
211 precuneus, displacing anteriorly/posteriorly the central area (Fig. 3). The proportions of the
212 paracentral lobule do not change. This change only influences brain landmarks and not skull
213 landmarks. Accordingly, along this vector, the relative position of the brain and cranial
214 references does change. The dilation (lengthening) of the precuneus mainly occurs anteriorly,
215 displacing the paracentral lobule towards a more forward position. Therefore, it involves a
216 reduction in the distance between the central cortical area and the bregma and, to a lesser
217 extent, increases the distance between the parietal lobes and the lambda. Hence, the position
218 of the cranial references (bones boundaries) relative to the cerebral references (lobes
219 boundaries) will depend upon the size of the parietal lobes. The rest of the spatial organization
220 is not particularly influenced by this main pattern. The result is the same if we analyze males
221 and females separately.

222 If we analyze only the outer profile (from the internal occipital protuberance to crista galli) or
223 only the cortical block (precuneus and paracentral lobule – Fig. 3d) the result is the same: a
224 first principal component associated with precuneal lengthening/shortening, in which this
225 change is particularly expressed forward, reducing/increasing the distance between the central
226 cortical area and the bregma.

227 A Partial Least-Square correlation between the central cortical block (precuneus and
228 paracentral lobule) and the rest of the configuration is not significant (p = 0.16), further
229 evidencing a lack of patent reciprocal association between these blocks.

230 In summary, we observe a modest correlation between parietal bone and lobe length, a large
231 individual variation, and a variable spatial organization between cranial and cerebral elements.
232 Variations of the brain proportions exert a minor influence on the extension of the vault
233 bones. The reciprocal position of cranial and cerebral elements is not constant, and their
234 morphology is sensitive to independent factors. The main pattern of variability is associated
235 with increase of the precuneus size, separating the boundaries between the parietal and
236 occipital bone and lobe, and approaching the boundaries between the frontal and parietal
237 bone and lobe.

238

6

239   **Discussion**

240

241   *The spatial relationships between brain and sutures*

242   The spatial relationships between brain and braincase represent a basic issue both in
243   evolutionary and medical studies. Previous pioneering analyses in neurosurgery have been
244   performed by dissection of cadavers (Ribas et al., 2006). However, analyses performed with
245   physical dissections have often limits in the sample size because of the difficulties in
246   performing these kinds of studies, and limits in the anatomical reliability because tissues are
247   not observed in their functional conditions. In this study, we analyze the geometric
248   relationships between major cranial and cerebral landmarks in a sample of 100 adult humans,
249   by using MRI imaging, bivariate analysis, and geometric morphometric multivariate
250   approaches. We computed a bivariate analysis to quantify the degree of correlation between
251   dimensions and position of the cortical and bone elements of the upper braincase. Then, we
252   computed a shape analysis to investigate the role of these relationships within the major
253   morphological schemes underlying the phenotypic structure.

254   The bivariate analysis showed that the correlation between parietal bones and lobes is very
255   weak. Larger lobes are associated with larger bones, but the correlation is low and there is a
256   considerable individual variability. In this sense, the null hypothesis is falsified because of the
257   existence of a correlation, and we can state that larger parietal lobes are associated with larger
258   parietal bones. However, this correlation is scanty, suggesting the existence of further
259   independent factors making this association feeble. The parietal lobes contribute to the
260   extension of the parietal bones, but only to a limited extent, at least when considering intra-
261   specific adult variability. In individuals with larger parietal lobes, the distance between the
262   boundaries of lobes (sulci) and bones (sutures) is smaller. Therefore, we can conclude that
263   there is an allometric pattern in which the enlargement of the parietal bone does not keep the
264   pace of the enlargement of the parietal lobe and, by consequence, the boundaries of these
265   two areas get closer. The pattern is however weak, influenced by other factors and by
266   individual variation. The fact that the two areas do not show a correspondent variation, and
267   the scarce correlation, suggest that the spatial position of the cranial and cerebral elements is
268   influenced by independent variables, with a limited integration between hard and soft tissues
269   in the final phenotype.

270   Shape analysis was aimed at considering whether these spatial relationships influence the
271   patterns of correlation which generate the phenotypic variation. In morphometrics, the
272   covariance structure as revealed through multivariate statistics is able to quantify and
273   characterize the strength of the correlation schemes constraining the phenotypic variability,
274   namely the degree and patterns of morphological integration among the anatomical
275   components (Wagner, 1984). Following these principles, studies in two (Bruner et al., 2010)
276   and three (Gómez-Robles, 2014) dimensions suggest that the adult brain morphology shows a
277   modest degree of integration, mostly based on local effects and physical proximity. Our data,
278   integrating the cranial component with the brain shape geometry, are in agreement with these
279   previous results, evidencing only one dominant pattern of covariance, followed by many minor

280   secondary vectors. This main pattern is associated specifically with the relative proportions of
281   the precuneus, displacing back and forth the paracentral lobule formed by the precentral and
282   postcentral areas. This same pattern has been described previously by using a different sample
283   (Bruner et al., 2014a), and that result can be confirmed and reproduced here. This change of
284   the precuneal area is not only a variation in parietal proportions compared with the rest of the
285   brain, but it is also associated with an actual enlargement/reduction of the precuneal cortical
286   surface (Bruner et al., 2015). The current analysis evidence that this major morphological
287   component, based on precuneus dimensions, involves brain geometry but without influencing
288   in a corresponding way the bone extension. Therefore, precuneus enlargement/reduction
289   changes secondarily the reciprocal positions of bones and lobes. The changes at the posterior
290   boundary are less conspicuous, most of the spatial adjustment being associated with the
291   displacement of the anterior areas. Once more, these results suggest independence between
292   the cranial and cerebral elements: as the brain proportions changes, the cranial boundaries do
293   not change accordingly. Interestingly, no endocranial morphological changes were described in
294   one case study in which a bregmatic bone was so large to constitute an actual fifth component
295   of the vault morphogenesis (Barberini et al., 2008). That case suggests a remarkable stability of
296   the endocranial morphological system, independent from patent changes of the suture
297   positions and patterns.

298   Therefore, we conclude that during morphogenesis the bulging of the parietal lobe can
299   influence the curvature of the parietal bone, but the spatial reciprocal organization of the
300   cranial and cerebral elements vary according to other independent factors. Hence, we must
301   probably distinguish a general *morphological integration* (form integration) from a more
302   specific *spatial integration* (relative position of the anatomical elements). It is worth noting
303   that the parietal enlargement associated with the braincase globularity of our species occurs in
304   a very early post-natal stage (Neubauer et al., 2009; Neubauer, 2014) and, beyond gross
305   morphological changes, the parietal cortex matures also very early (Gogtay et al., 2004). In
306   later stages other brain and cranial districts undergo growth and development, changing the
307   spatial relationships previously established (Bastir et al., 2006). With this information in mind,
308   at least two different hypotheses can explain the partial independence between cranial and
309   cerebral elements that we have described in this study among adult individuals: the changes of
310   the spatial relationships between parietal bones and lobes can be achieved during the parietal
311   morphogenesis, or else after this stage (Fig. 4). In the first case, the parietal bulging associated
312   with the globularization stage specific of our species would change the spatial relationships
313   between bones and lobes. The growing parietal volume displaces the frontal cortex, and the
314   central sulcus approaches the frontal bone. In the second case, the parietal bulging would be
315   associated with a corresponding (isometric) growth of the parietal bone. In this stage, there is
316   a tighter integration between parietal bone and lobe. Such correspondence is then lost in
317   successive stages, when the anterior areas (the frontal lobes and the facial block) grow and
318   develop during later morphogenetic steps. Ontogenetic series will be necessary to evaluate
319   these two alternatives.

320

321   *Parietal enlargement and paleoneurology*

322

323 Bregma and lambda are the boundaries between the frontal, parietal, and occipital bones. The
324 central sulcus and the perpendicular sulcus are the boundaries between the frontal, parietal,
325 and occipital lobes. While bones are real biological units associated with specific
326 morphogenetic elements, lobes are conventional units, which do not represent actual
327 neuroanatomical entities. Nonetheless, the correspondence between bones and lobes is often
328 used as a possible reference in medicine and paleoneurology. In surgery, cranial landmarks are
329 used as spatial reference to plan and perform operations. In paleoneurology, cranial landmarks
330 are used to estimate brain areas. In neurosurgery, current biomedical imaging is a form of
331 direct support to develop and verify a proper map of the relationships between skull and brain
332 anatomy. In contrast, in paleoneurology, the soft tissues are lost, and brain shape can be only
333 inferred by using endocranial shape. The current analysis suggests that in modern humans
334 cranial sutures should not be used as fixed references to make inferences on brain areas, at
335 least according to their specific position. In this sense, "average" distances between brain and
336 skull landmarks may not be informative and may be even misleading, because they do not
337 consider the reciprocal variations of these elements. The overall form of the brain surface (that
338 is, its size and shape) can actually be extrapolated from the endocranial form, because brain
339 growth molds the neurocranial bones directly, most of all at the vault (Moss and Young, 1960;
340 Enlow, 1990). Furthermore, the correspondence between brain morphology and endocranial
341 surface, although not complete, is also sufficiently reliable to localize major anatomical cortical
342 traits on endocasts (Kobayashi et al., 2014a). In contrast, the specific extension of the cortical
343 areas should not be inferred or extrapolated directly from the position of the cranial
344 boundaries alone.

345 Quantitative scaling rules derived from the observed variation of relative spatial positions, like
346 in the present analysis, could be used to extrapolate brain landmarks from cranial landmarks.
347 Nonetheless, the current study evidences that, beyond such a lack of fixed proportions
348 between bones and lobes boundaries, there is also an important individual variation
349 suggesting that multiple factors are involved in the final phenotype. In adult modern humans,
350 the length of the parietal bone is influenced by the size of the parietal lobes to a very minor
351 extent (7-10%), and this value is even lower when accounting only for the length of the
352 precuneus (4-6%). Arcs displayed larger correlations than chords, revealing a role of the
353 bulging effect, but the increase of variance explained is however scanty (2-3%). This means
354 that, even if the parietal lobe moulds the shape and surface of the parietal bone (Moss and
355 Young, 1960), it influences its longitudinal extensions to a much minor degree. Correlations at
356 inter-specific level are often more pronounced than at intra-specific level, and therefore we
357 may expect that this value, when comparing different hominids, may be larger. It must be in
358 fact evidenced that this result refers to intra-specific adult variation. Intra-specific and inter-
359 specific correlation patterns can be based on very different mechanisms, the former being the
360 result of normal variation, and the latter of specific adaptations (Martin and Barbour, 1989).
361 Integration, pleiotropy, and poligeny create important connections between intra- and inter-
362 specific variability (e.g., Cheverud 1982, 1996). However, results in one of these two domains
363 should not be strictly intended as results in the other. In this sense, studies in comparative

364 primatology will be necessary to evaluate whether the patterns observed in the current
365 analysis can be extended beyond the species-specific limits. For example, macaques display
366 more stable relationships between cranial and cerebral references, at least when considering
367 the coronal suture and cortical references associated with parasagittal elements of the frontal
368 lobes (Kobayashi et al., 2014b). A similar consideration must be put forward when considering
369 static variation (that is adult variation, such as in this study) versus ontogenetic variation.
370 Nonetheless, without this information, we must take into account that vault bones and brain
371 lobes may share shape (curvature) and surface morphology (sulcal traits), but the reciprocal
372 position of their anatomical boundaries and extension is more variable and less reliable.

373 The shape variations described here are particularly important when considering that the
374 precuneal changes responsible for modern human brain variability are very similar to the
375 pattern of cranial variation associated with the modern human skull evolution (Bruner et al.,
376 2014b). These two patterns are so comparable to suggest a relationship between intra-specific
377 and inter-specific variations. When compared with other hominids, *Homo sapiens* displays a
378 distinct and specific increase of the parietal bone diameters (Bruner et al., 2011). Hence, the
379 pattern described in this study, responsible for the changes in the distances between bones
380 and lobes, may be the same involved in generating cranial differences between modern and
381 non-modern humans.

382 Non-modern human species lacked the parietal bulging described in modern humans, possibly
383 even presenting a negative allometric trend: the larger the brain, the relatively shorter the
384 parietal areas (Bruner, 2004). If the mismatch between brain and skull landmarks described in
385 this study is also effective at evolutionary level, we must infer that Neanderthals, having the
386 largest cranial capacity among non-modern human species, probably displayed extreme values
387 along this morphological vector. That is, Neanderthals may have had the bregma which was
388 more distant from the central sulcus compared with modern humans.

389 The parietal bone and the occipital bone are strongly integrated, and the bulging of one of
390 these areas is associated with the flattening of the other (Gunz and Harvati, 2007).
391 Interestingly, in Neanderthals, the relative shortening of the parietal areas, possibly related to
392 encephalization and parietal constraints in the human genus, is associated with lambdatic
393 supernumerary ossicles, suggesting a degree of morphogenetic imbalance in those areas
394 (Manzi et al, 1996; Bruner, 2014). Taking into account the pattern described in this article, we
395 may wonder whether such lack of reciprocal adjustment between brain and skull references,
396 associated with structural limits of a large brain size and the integration between the parietal
397 and occipital bones, may be involved in those constraints and consequent morphological
398 instability.

399

400 **Conclusions**

401

402 Paleoneurology aims to reconstruct brain form in fossil species, by analyzing their endocranial
403 anatomy (Holloway et al., 2004). Unfortunately, cortical imprints on the endocranial surface
404 may be very faint, and much experience is needed to reveal cortical patterns on the
405 endocranial mould. Generally, multiple sources of information are necessary to make such
406 inferences, integrating metric and non-metric inputs from the neighboring cranial and
407 endocranial characters. Despite such uncertainty, endocranial morphology is the only direct
408 evidence of brain change in evolutionary neuroanatomy, and we should try to optimize this
409 resource. This study evidences that, at least when considering the adult intra-specific variation,
410 the spatial correlation between cranial and cerebral elements is scarce. The main source of
411 morphological variation, i.e. the size of the precuneus, alters the reciprocal position of neural
412 and cranial elements. Although the proportions of the parietal lobes are probably crucial in
413 shaping the brain phenotype in both ontogenetic and phylogenetic terms (Bruner et al.,
414 2014a,b, 2015), its extension shows only a weak correlation with the extension of the parietal
415 bone. Local influences and multiple factors associated with a non-linear morphogenetic
416 process based on different and independent stages are probably the reason of such lack of
417 strict correspondence in the position of hard and soft tissues. The lack of strong integration
418 patterns makes any relationship between cerebral and neurocranial boundaries feeble. Scaling
419 rules can be tentatively investigated to evaluate how those boundaries can vary according to
420 the variation of specific brain areas such as, in this case, the parietal cortex. Although brain and
421 braincase shows a reciprocal relationship in terms of size (volume) and shape (curvature), the
422 position of their anatomical elements is sensitive to independent factors. This independence
423 must be necessarily considered when evaluating brain reconstruction in fossil species.

424

425 **Acknowledgments**

426

439

440 **References**

441

442   **Aldridge K, Marsh JL, Govier D, Richtsmeier JT** (2002). Central nervous system phenotypes in
443   craniosynostosis. *J Anat* **201**, 31-39.

444   **Barberini F, Bruner E, Cartolari R, et al.** (2008) An unusually-wide human bregmatic Wormian
445   bone: anatomy, tomographic description, and possible signifcance. *Surg Radiol Anat*
446   **30,** 683–687.

447   **Bastir M, Rosas A** (2005) Hierarchical nature of morphological integration and modularity in
448   the human posterior face. *Am J Phys Anthropol* **128,** 26-34.

449   **Bastir M, Rosas A, O'Higgins P** (2006) Craniofacial levels and the morphological maturation of
450   the human skull. *J Anat* **209,** 637-654.

451   **Bookstein FL** (1991) *Morphometric Tools for Landmark Data: Geometry and Biology*.
452   Cambridge: Cambridge University Press.

453   **Bookstein FL, Gunz P, Mitteroecker P, et al.** (2003) Cranial integration in *Homo*: singular warps
454   analysis of the midsagittal plane in ontogeny and evolution. *J Hum Evol* **44,** 167-187.

455   **Bruner E** (2004) Geometric morphometrics and paleoneurology: brain shape evolution in the
456   genus *Homo*. *J Hum Evol* **47,** 279-303.

457   **Bruner E** (2014). Functional craniology, human evolution, and anatomical constraints in the
458   Neanderthal braincase. In: Akazawa T., Ogihara N., Tanabe H.C., & Terashima, H. (eds.),
459   Dynamics of Learning in Neanderthals and Modern Humans (Vol. 2), pp. 121–129.
460   Japan: Springer.

461   **Bruner E** (2015) Functional craniology and brain evolution. In: *Human Paleoneurology* (ed.
462   Bruner E.), pp. 57-94. Springer International Publishing.

463   **Bruner E, Ripani M** (2008) A quantitative and descriptive approach to morphological variation
464   of the endocranial base in modern humans. *Am J Phys Anthropol* **137,** 30–40.

465   **Bruner E, Saracino B, Ricci F, et al.** (2004) Midsagittal cranial shape variation in the genus
466   *Homo* by geometric morphometrics. *Coll Antropol* **28,** 99-112.

467   **Bruner E, Martin-Loeches M, Colom R** (2010) Human midsagittal brain shape variation:
468   patterns, allometry and integration. J Anat **216,** 589–599.

469   **Bruner E, de la Cuétara JM, Holloway R** (2011) A bivariate approach to the variation of the
470   parietal curvature in the genus *Homo*. *Anat Rec* **294,** 1548-1556.

471   **Bruner E, Rangel de Lázaro G, de la Cuétara JM, et al.** (2014a). Midsagittal brain variation and
472   shape analysis of the precuneus in adult humans. *J Anat* ***224,*** 367-376.

473   **Bruner E, de la Cuétara JM, Masters M, Amano H, Ogihara N** (2014b) Functional craniology
474   and brain evolution: from paleontology to biomedicine. *Frontiers in neuroanatomy* **8.**

475 **Bruner E, Román FJ, de la Cuétara JM, Martin-Loeches M, Colom R.** (2015). Cortical surface
476   area and cortical thickness in the precuneus of adult humans. *Neuroscience* **286**, 345-
477   352.

478 **Cheverud JM** (1982) Relationships among ontogenetic, static, and evolutionary allometry. *Am J*
479   *Phys Anthropol* **59,** 139–149.

480 **Cheverud JM** (1996) Developmental integration and the evolution of pleiotropy. *Am Zool* **36,**
481   44–50.

482 **Cotton F, Rozzi FR, Vallee B, et al.** (2005) Cranial sutures and craniometric points detected on
483   MRI. *Surg Radiol Anat* **27,** 64-70.

484 **Enlow DH** (1990) *Facial growth*. Philadelphia: Saunders.

485 **Gogtay N, Giedd JN, Lusk L, et al.** (2004) Dynamic mapping of human cortical development
486   during childhood through early adulthood. *Proc Natl Acad Sci U.S.A.* **101,** 8174-8179.

487 **Gómez-Robles A, Hopkins WD, Sherwood CC** (2014) Modular structure facilitates mosaic
488   evolution of the brain in chimpanzees and humans. *Nature communications* **5.**

489 **Gunz P, Harvati K** (2007) The Neanderthal "chignon": variation, integration, and homology. *J*
490   *Hum Evol* **52**, 262–274.

491 **Hammer Ø, Harper DAT, Ryan PD** (2001) PAST: paleontological statistics software package for
492   education and data analysis. *Paleontol Electronica* **4,** 1–9.

493 **Hilgetag CC, Barbas H** (2005) Developmental mechanics of the primate cerebral cortex. *Anat*
494   *Embryol* **210,** 411-417.

495 **Holloway RL, Broadfiled DC, Yuan MS** (2004) *The human fossil record, Vol. 3: Brain endocast*.
496   Hoboken: Wiley.

497 **Jiang X, Iseki S, Maxson RE, Sucov HM, Morriss-Kay GM** (2002) Tissue origins and interactions
498   in the mammalian skull vault. *Develop Biol* **241**, 106-116.

499 **Klingenberg CP** (2011) MorphoJ: an integrated software package for geometric
500   morphometrics. *Mol Ecol Resour* **11,** 353–357.

501 **Kobayashi Y, Matsui T, Haizuka Y, Ogihara N, Hirai N, Matsumura G.** (2014a) Cerebral sulci
502   and gyri observerd on macaque endocasts. In: Akazawa T., Ogihara N., Tanabe H.C., &
503   Terashima, H. (eds.), Dynamics of Learning in Neanderthals and Modern Humans (Vol.
504   2), pp. 131–137. Japan: Springer.

505 **Kobayashi Y, Matsui T, Haizuka Y, Ogihara N, Hirai N, Matsumura G.** (2014b) The coronal
506   suture as an indicator of the caudal border of the macaque monkey prefrontal cortex.
507   In: Akazawa T., Ogihara N., Tanabe H.C., & Terashima, H. (eds.), Dynamics of Learning
508   in Neanderthals and Modern Humans (Vol. 2), pp. 139–143. Japan: Springer.

509 **Manzi G, Vienna A, Hauser G** (1996) Developmental stress and cranial hypostosis by
510   epigenetic trait occurrence and distribution: an exploratory study on the Italian
511   Neandertals. *J Hum Evol* **30**, 511–527.

512 **Marcus DS, Wang TH, Parker J, et al.** (2007) Open Access Series of Imaging Studies (OASIS):
513   cross-sectional MRI data in young, middle aged, nondemented, and demented older
514   adults. *J Cognitive Neurosci* **19,** 1498-1507.

515 **Martin RD, Barbour AD** (1989) Aspects of line-fitting in bivariate allometric analyses. *Folia*
516   *Primatol* **53,** 65–81.

517 **Mitteroecker P, Bookstein F** (2008) The evolutionary role of modularity and integration in the
518   hominoid cranium. *Evolution* **62**, 943-958.

519 **Morriss-Kay GM, Wilkie AO** (2005) Growth of the normal skull vault and its alteration in
520   craniosynostosis: insights from human genetics and experimental studies. *J Anat* **207**,
521   637-53.

522 **Moss ML, Young RW** (1960) A functional approach to craniology. *Am J Phys Anthropol* **18,** 281–
523   292.

524 **Neubauer S** (2014) Endocasts: possibilities and limitations for the Interpretation of human
525   brain evolution. *Brain Behav Evol* 84, 117–134.

526 **Neubauer S, Gunz P, Hublin JJ** (2009) The pattern of endocranial ontogenetic shape changes in
527   humans. *J Anat* **215,** 240–255.

528 **Ogihara N, Amano H, Kikuchi T, et al.** (2015). Towards digital reconstruction of fossil crania
529   and brain morphology. *Anthropol Sci* (in press).

530 **Ribas GC, Yasuda A, Ribas EC, Nishikuni K, Rodrigues AJ Jr** (2006) Surgical anatomy of
531   microneurosurgical sulcal key-points. *Neurosurgery* **59,** S177-S208.

532 **Richtsmeier JT, Aldridge K, de Leon VB, et al.** (2006) Phenotypic integration of neurocranium
533   and brain. *J Exp Zool B Mol Dev Evol* **306B**, 360–378.

534 **Rohlf FJ, Corti M** (2000) The use of two-block partial least squares to study covariation in
535   shape. *Syst Biol* **49**, 740–753.

536 **Van Essen DC** (1997) A tension-based theory of morphogenesis and compact wiring in the
537   central nervous system. *Nature* **385,** 313-318.

538 **Wagner GP** (1984) On the eigenvalue distribution of genetic and phenotypic dispersion
539   matrices: evidence for a nonrandom organization of quantitative character variation. *J*
540   *Math Biol* 21, 77–95.

541 **Zelditch M, Swiderski D, Sheets D, Fink W** (2004) Geometric Shape Analysis for Biologists: A
542   Primer. San Diego: Elsevier.

543

544

545

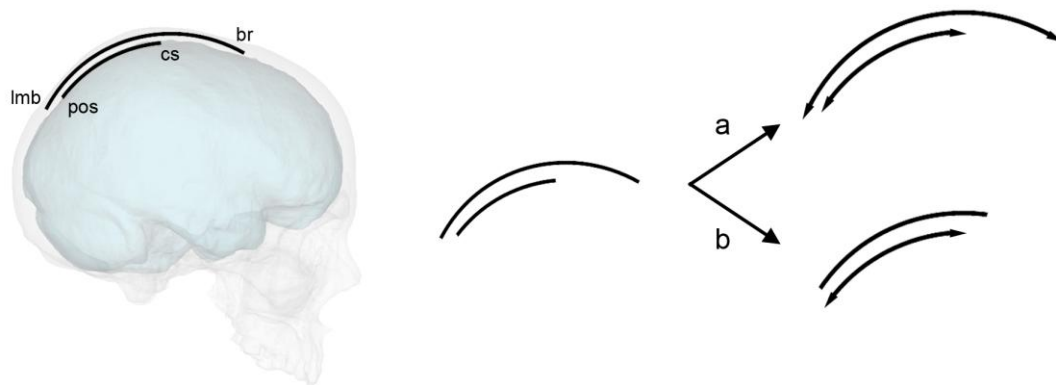546   **Table 1.** Distribution of the inter-landmark distances (mm.)

547

|	Mean	St. Dev.	25º	Median	75º
Bregma-Central sulcus	57.9	6.8	54.0	57.3	61.5
Lambda-Perpendicular sulcus	10.1	6.9	5.7	10.3	14.5
Parietal bone length	114.2	5.8	109.8	114.2	118.8
Parietal lobe length	56.6	7.3	51.5	56.8	61.3
Precuneus length	37.0	7.6	31.3	37.3	41.4

548

549

550

551

552 **Figure 1.** Parietal bones and parietal lobes share morphogenetic processes, displaying a
553 correspondence in terms of curvature and size. However, we ignore whether larger lobes
554 involve proportional larger bone (a) or else if their respective boundaries are not sensitive to
555 reciprocal variations (b). Position of lambda (lmb), bregma (br), central sulcus (cs) and parieto-
556 occipital sulcus (pos) are here approximate for graphic purposes.

557

558
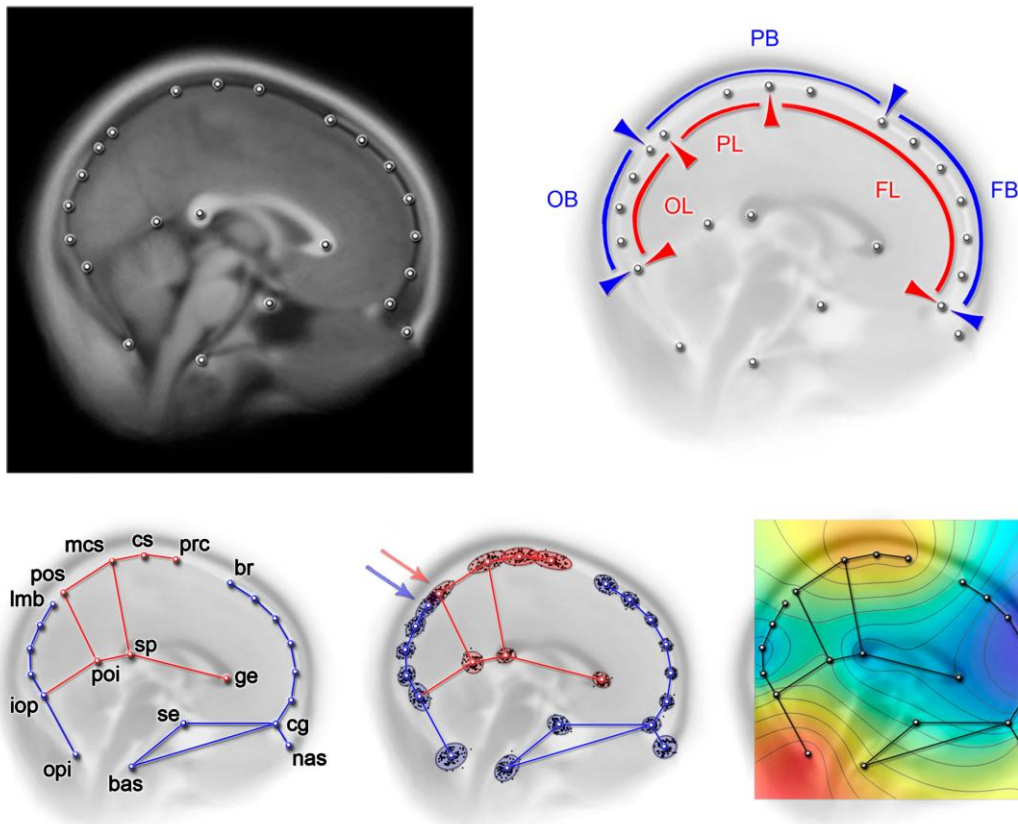
559

560 **Figure 2.** In the upper row, configuration of landmarks used in this analysis plotted on the
561 mean superimposed images from the whole sample, displaying the average brain midsagittal
562 morphology (left) and showing the spatial relationships between frontal, parietal, and occipital
563 lobes (FL, PL, OL) and bones (FB, PB, OB). In the lower row, landmark with labels (red: brain
564 landmarks; blue: cranial landmarks; unlabelled landmarks: semilandmarks)(left), scatterplot
565 after Procrustes superimposition (center), and map of residual variation after registration (red:
566 high; blue: small)(right). Labels - bas: basion; br: endobregma; cg: crista galli; cs: central sulcus;
567 ge: genu; iop: interna occipital protuberance; lmb: endolambda; mcs: marginal ramus of the
568 cingulate sulcus; nas: nasion; opi: opistion; poi: parieto-occipital sulcus (internal); pos: parieto-
569 occipital sulcus (external); prc: precentral sulcus; se: sella; sp: splenium. The arrows show the
570 overlapping of the parieto-occipital sulcus (perpendicular scissure) and endolambda. Cranial
571 and brain landmarks were sampled on the endocranial surface, independently upon minor
572 differences due to meningeal thickness, which is nonetheless negligible and not properly
573 visible at the current resolution.

574

575

576
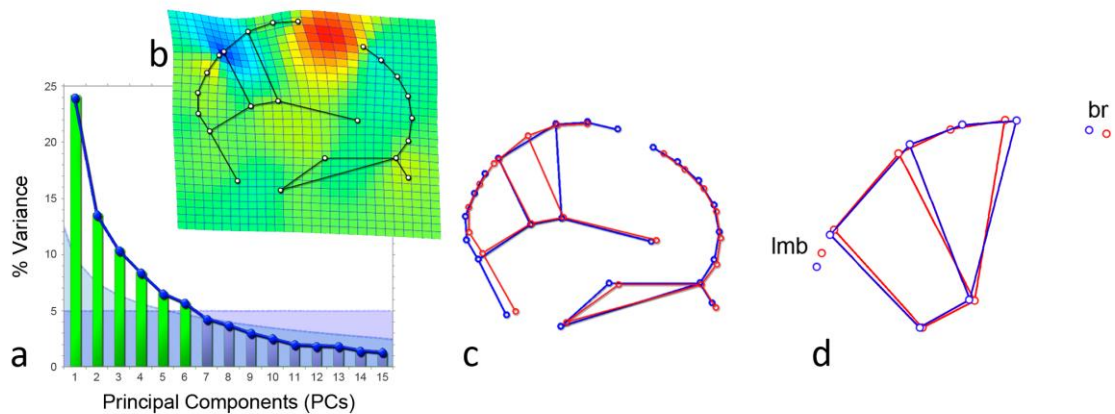
577

578 **Figure 3.** a) scree plot of the Principal Component Analysis, showing in green the components
579 beyond the broken stick threshold (blue curve) and the 5% variance (violet area); b)
580 deformation grid show the changes associated with the first component, with expansion
581 factors (red: dilation; blue: compression); c) the same pattern showed by wireframes; d)
582 wireframes for the principal component when considering only precuneus, paracentral lobule,
583 bregma (br), and lambda (lmb).

584
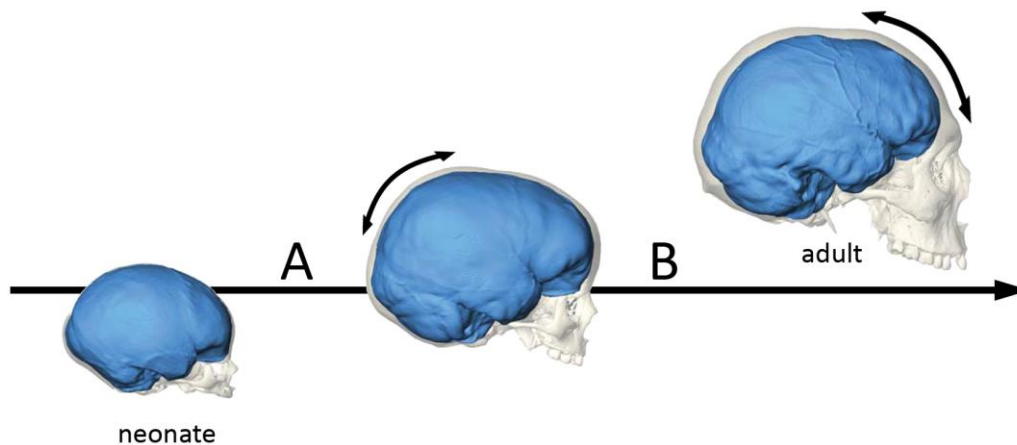
585

586

587 **Figure 4.** Parietal bulging in modern humans occurs in the early postnatal stage (A), while
588 frontal and facial morphology undergo changes in successive ontogenetic steps (B). The spatial
589 dissociation between cerebral and cranial elements can be the result of the early parietal
590 growth. Alternatively, parietal bones and lobes can be more integrated during this stage, but
591 the spatial association can be lost in the successive steps, after modification of the frontal and
592 facial blocks (digital reconstructions after Neubauer, 2014).